

Voltage-Induced Dependence of Raman-Active Modes in Single-Wall Carbon Nanotube Thin Films

Giovanni Fanchini,* Husnu Emrah Unalan, and Manish Chhowalla

Materials Science and Engineering, Rutgers University, Piscataway, New Jersey 08854

Received October 13, 2006; Revised Manuscript Received February 9, 2007

ABSTRACT

We report on electrical Raman measurements in transparent and conducting single-wall carbon nanotube (SWNT) thin films. Application of external voltage results in downshifts of the D and G modes and in reduction of their intensity. The intensities of the radial breathing modes increase with external electric field related to the application of the external voltage in metallic SWNTs, while decreasing in semiconducting SWNTs. A model explaining the phenomenon in terms of both direct and indirect (Joule heating) effects of the field is proposed. Our work rules out the elimination of large amounts of metallic SWNTs in thin film transistors using high field pulses. Our results support the existence of Kohn anomalies in the Raman-active optical branches of metallic graphitic materials.

Transparent and conducting single-wall carbon nanotube (SWNT) thin films are two-dimensional, low-density networks of SWNTs¹ which are interesting both fundamentally and technologically. Recently, it has been noticed² that the Drude relaxation times in SWNT thin films, and therefore their optoelectronic properties, are controlled by intertube processes. This is an important difference with respect to individual SWNTs where intratube processes dominate.³ The intertube processes in SWNT thin films arise from the tube to tube transport because the distance between the electrodes ($\sim 20 \mu\text{m}$) is typically much larger than the SWNT length. The transport properties in these networks can be explained by the percolation theory.¹

Technologically, the ability to tailor the optical absorption coefficient and conductivity of SWNT thin films over several orders of magnitude makes them attractive for transparent and flexible electronics.^{4–7} During SWNT thin film transistor fabrication, it is a common practice to precondition the SWNT network using high voltage pulses to improve the on/off ratio through supposed preferential elimination of metallic SWNTs by Joule heating.^{4–7} This effect is claimed on the basis of the decrease in channel conductivity and a similar effect occurring in individual SWNTs, but little information on the modifications of the SWNTs in thin films after voltage application is available and a Raman study is still lacking.

In this Letter, we report on the Raman measurements of SWNT thin films recorded under external voltages. We have found that, although the conductivity strongly decreases, the changes in the Raman peaks are to the largest extent reversible. The films were deposited on glass using the

method of Wu et al.⁸ from 10, 30, and 50 mL of a 2 mg/L suspension of purified HiPCO SWNTs.^{2,9} Gold electrodes (width 1 mm, distances 20 and 60 μm) were defined on each substrate. External voltages of 0–15 V (leading to electric fields $E_{\text{ext}} = 0\text{--}7500 \text{ V cm}^{-1}$) were applied during the Raman measurements using a GW GPS-1850D power supply. The spectra were recorded in air on a Renishaw InVia spectrometer. Our setup for electrical Raman measurements is presented in Figure 1a. Low laser powers (12.5 $\mu\text{W}/\mu\text{m}^2$ at 1.96 eV excitation, 25 $\mu\text{W}/\mu\text{m}^2$ at 1.57 eV) were used and tested to not produce laser heating. The current was simultaneously monitored using a Keithley 195A multimeter. Each series of Raman spectra at the varying voltage was recorded on the same spot in order to attain comparable signal intensity. After any measurement at a given external field, sufficiently low field (500 V/cm, leading to undetectable changes in the Raman signal) was applied so that a low-field Raman spectrum and the sample conductance could be recorded.

The typical variation of the G-bands³ and the doubly resonant D-band¹⁰ under the influence of an electric field are shown in parts b and c of Figure 1, respectively. A clear decrease in peak position (Ω) and intensity (I_S) for both bands with increasing electric field (E_{ext}) can be observed. Similar shifts in the Raman bands under the influence of electric fields have been observed in ferroelectrics.¹¹ In contrast, electrochemical Raman measurements of SWNT electrodes in aqueous environments¹² resulted in upshifts of the G-bands, which clearly points to differences between our and such experiments. Electromechanical Raman measurements may lead to both upshifts or downshifts.¹³

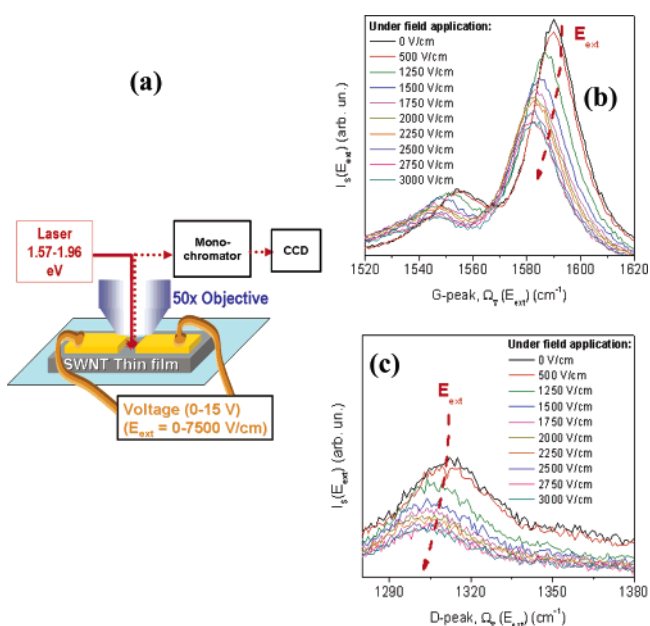


Figure 1. (a) Schematic of the setup for electrical Raman measurements. Typical dependence of the Raman modes on the electric field (E_{ext}) (b) for the G peak (excitation energy $\hbar\omega = 1.96$ eV) and (c) for the D peak. From panels b and c, the two main effects, peak downshifts and decrease in peak intensities, are evident.

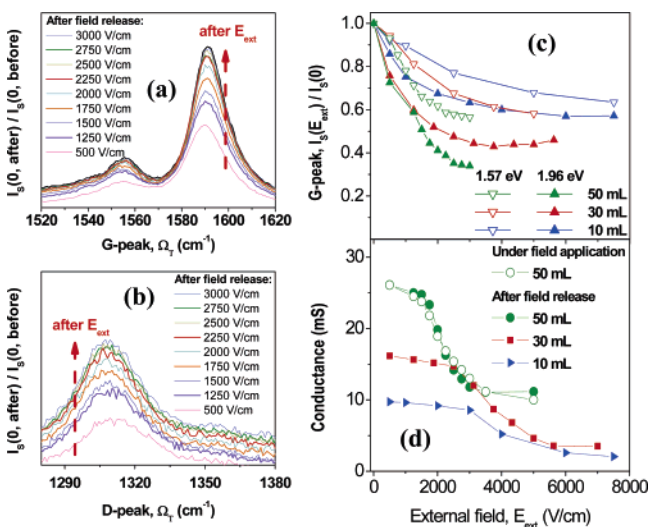


Figure 2. Permanent increase of the low-field intensities of (a) the G peak and (b) the D peak. Data in panels a and b are recorded at the same runs as panels b and c of Figure 1. (c) Dependence of the Raman G-peak intensities on the electric field (E_{ext}). (d) Permanent decrease in sample conductance is measured, and it does not recover after the electric field is released.

77 Parts a and b of Figure 2 show the Raman peaks recorded
 78 immediately after releasing each external field used for the
 79 measurements shown in parts b and c of Figure 1. The
 80 recovery of the G and D peaks to their original frequencies
 81 is evident. Peak intensities not only recover but also increase
 82 slightly compared to their pristine value before field ap-
 83 plication. From the data in Figure 2a,b we conclude that the
 84 observed effects on the G and D peaks are indeed reversible.
 85 The data from Figures 1b and 2a are summarized in Figure
 86 2c, showing the ratios between the intensity of the G-bands

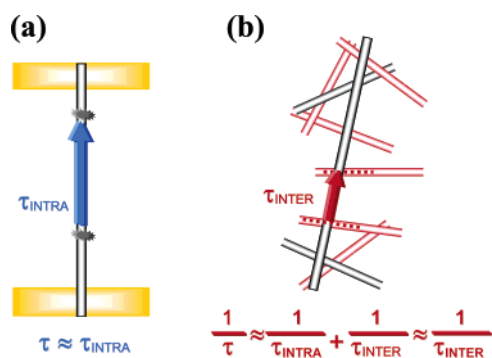


Figure 3. Schematics of (a) intratube processes (mostly related to electron–phonon interaction) and (b) intertube processes (related to cross links of different SWNTs) in determining relaxation times. Intratube processes control the performance of individual SWNTs. Intertube processes prevail in SWNT films where each m-SWNT (depicted in black) is cross linked by many other nanotubes, including semiconducting ones (depicted in red).

before and after the external field release for the samples
 and excitation energies investigated in this study.

While the Raman effects in our experiments are reversible,
 the conductance does not recover after the external field
 release (Figure 2d). Similar decrease in conductance has been
 found to improve the on/off ratio of thin film transistors and
 claimed to be due to burning of metallic SWNTs.^{4–7} In our
 study, the reversibility in decrease of the peak intensities
 rules out the burning of large amounts of SWNTs. We
 corroborate this by analyzing the radial breathing mode
 (RBM) of (n,m) -SWNTs in our films, as discussed below.

It is tempting to assign the observed downshifts to voltage-
 induced Joule heating, increasing the temperature of the
 films. Although alternative hypotheses can be easily dis-
 missed,¹⁴ it is crucial to clarify the origin and the amount of
 Joule heating itself, which must be expectedly large in order
 to justify the observed behavior. It was calculated¹⁵ that
 strong selective heating of Raman-active phonon modes (up
 to $T \sim 10^4$ K in *individual* metallic SWNTs) occurs in the
 presence of current due to Kohn anomalies.¹⁶ Figure 1,
 however, shows that the linewidth of the G and D bands
 does not appreciably increase with electric field, as it would
 do in the presence of a strong increase in phonon tempera-
 ture. Therefore, we will discuss our results in terms of moderate
 Joule heating in the presence of Kohn anomalies in an
 adiabatic system dominated by intertube interactions. This
 leads to strong electric-field-dependent fluctuations in the
 dielectric response of SWNT films, with the same mechanism
 leading to fluctuations of the Raman frequencies in ferro-
 electrics.¹¹

Let us first recall that in percolating SWNT networks, the
 electronic confinement is released and the wave functions
 extend over several SWNTs, both semiconducting (s-
 SWNTs) and metallic (m-SWNTs), and τ , the Drude
 relaxation times, depend on the network density and not on
 intrinsic properties of SWNTs.² The intra- and intertube
 processes for an individual SWNT and a network of SWNTs
 are schematically shown in Figure 3a,b. In a system where
 both intra- and interparticle processes contribute to the
 transport mechanisms and the relaxation of electron mo-

127 menta, the effective relaxation time can be written according
128 to Matthiessen's rule¹⁷ as

$$\frac{1}{\tau} = \frac{1}{\tau_{\text{INTRA}}} + \frac{1}{\tau_{\text{INTER}}} \quad (1)$$

129 where τ_{INTRA} and τ_{INTER} represent the intratube and intertube
130 relaxation times, respectively. Therefore, τ is dominated by
131 the shorter of τ_{INTRA} or τ_{INTER} which, in SWNT thin films
132 where each tube is interconnected to many others, is clearly
133 the latter. Relaxation indicates that the external field displaces
134 the Fermi sphere through a shift in momentum $\hbar\Delta k$ ¹⁸

$$\hbar\Delta k = e\tau \cdot E_{\text{ext}} \quad (2)$$

135 where e is the electron charge.

136 Let us now recall that the strong Raman activity of the G
137 and D bands of metallic SWNTs should correspond to
138 exceptionally strong electron-phonon coupling,^{3,10,19} whose
139 origin had been unclear for a long time. Recently, Piscanec
140 et al.¹⁶ offered an explanation through demonstration of the
141 existence of Kohn anomalies in the screening of ions in
142 metallic graphitic materials. In general, Kohn anomalies
143 occur when the size of the Fermi surface is comparable to
144 the phonon wavevector \mathbf{q} .^{16,20-22} As discussed by Piscanec
145 et al.,¹⁶ the π and π^* bands in graphite and m-SWNTs touch
146 the Fermi level (E_F) at the \mathbf{K} -point which results in a very
147 small Fermi wavevector ($\mathbf{k}_F \sim \mathbf{0}$) whose modulus approaches
148 those of the G and D phonon wavevectors ($\mathbf{q} = \mathbf{\Gamma} = \mathbf{0}$ and
149 $\mathbf{q} = \mathbf{q}' - \mathbf{K} = \mathbf{0}$). Since $|2\mathbf{k}_F|^{-1}$ represents the typical scale
150 length for screening a pointlike disturbance,²² the condition
151 $\mathbf{q} \sim 2\mathbf{k}_F \sim \mathbf{0}$ requires that infinite distance is needed for the
152 electrons to fully screen an optical phonon.

153 It is well-known that Kohn anomalies in one-dimensional
154 (1-D) solids lead to logarithmic divergence of the static
155 dielectric response, $\epsilon(q \sim 2k_F, \hbar\omega \sim 0)$, while in 3-D solids
156 the divergence only affects the first derivative of this quantity.
157 Dealing with 1-D electronic structures, it is then obvious
158 that small fluctuation in the electron momenta (e.g., by
159 applying a constant external field) corresponds to strong, non-
160 negligible, fluctuation in the dielectric response.²³ We shall
161 treat such fluctuations in the framework of the Lindhard
162 model.²⁴ Accordingly, the dynamic dielectric response of the
163 anomalously screening electrons in the presence of a change
164 in momentum $\hbar\Delta k(E_{\text{ext}})$ is given by²²

$$\begin{aligned} \epsilon[\Delta k(E_{\text{ext}}), \hbar\omega] - 1 = \\ -4e^2\epsilon_0 \lim_{\substack{k_F \rightarrow 0 \\ q/2k_F \rightarrow 1}} \int dk \frac{f(k_F + \Delta k + q/2, T) - f(k_F + \Delta k - q/2, T)}{\epsilon_{k+\Delta k+q/2} - \epsilon_{k+\Delta k-q/2} - \hbar\omega} \end{aligned} \quad (3)$$

165 where ϵ_0 is the dielectric response in vacuum and the Fermi-
166 Dirac population probability $f(k, T)$ will be taken to be
167 approximately linear in the energy domain $E_F \pm k_B T/2$ and
168 1 or 0 elsewhere. Since the dielectric responses obtained from
169 ellipsometry at our Raman excitation energies ($\hbar\omega = 1.57-$

1.92 eV) follow a Drude behavior,² ϵ_k will be taken to be
the dispersion relation for free electrons ($\epsilon_k = \hbar^2 k^2/2m$).
Similar conclusions however can be also anticipated when
assuming a linear band structure for ϵ_k as customary for
individual SWNTs. Care should be taken in evaluating eq
3, because very slight changes in q , ω , and T can lead to
fluctuations of $\epsilon(q, \hbar\omega)$ from 1 to infinity.²³ Therefore, since
a very small value of k_F is expected in our percolating
networks, we estimate eq 3 at k_F tending to zero with the
same zeroth order of q , thus leading to a finite ratio $q/2k_F$
 $\rightarrow 1$. Evaluation of eq 3 gives $\epsilon(0, \hbar\omega > 0) - 1 = 0$ in the
absence of electric field, while in the presence of field

$$\begin{aligned} \epsilon(\Delta k, \hbar\omega) - 1 = \\ \frac{8e^2}{\epsilon_0 k_B T} \left(\sqrt{\frac{mk_B T}{\hbar^2} + \Delta k^2} - \sqrt{\frac{mk_B T}{\hbar^2} - \Delta k^2} \right) \end{aligned} \quad (4)$$

for

$$k_B T \gg \frac{\hbar^2 \Delta k^2}{m}$$

183 The intensity and the frequency of the Raman-active
184 optical phonons are related, via the electron-phonon cou-
185 pling, to the dynamic dielectric response $\epsilon(q \sim 2k_F, \hbar\omega)$.²²
186 Therefore, knowledge of the dynamic dielectric response will
187 now allow us to extract information about the G and D mode
188 frequencies. Especially, if the screening is assumed to
189 (perturbed by temperature and electric field) largely deter-
190 mine frequencies of the screened optical phonons, then the
191 Raman shifts in the presence [$\Omega(E_{\text{ext}})$] and absence [$\Omega(0)$]
192 of field can be related by^{11,25}

$$\Omega_T(E_{\text{ext}})^2 \cdot \epsilon[\Delta k(E_{\text{ext}}), \hbar\omega] = \Omega_T(0)^2 \cdot \epsilon(0, \hbar\omega) \quad (5)$$

193 The anharmonic modifications of the SWNT structure can
194 be included by assuming a temperature-dependent zero-field
195 Raman shift $\Omega_T(0) \approx \Omega_{300\text{K}}(0) - X_T T$ ($X_T \approx 0.01 \text{ cm}^{-1} \text{ K}^{-1}$,
196 for the G peak²⁶). However, we anticipate that they would
197 not significantly affect the parameters achievable by fitting
198 our model with the experiment (relaxation times and tem-
199 peratures change below 30-40%). Replacement of
200 $\epsilon[\Delta k(E_{\text{ext}}), \hbar\omega]$ and $\epsilon(0, \hbar\omega)$ from eqs 3 and 4 into eq 5 leads
201 to the following relation for the frequency of the Raman
202 optical modes upon temperature and external field increase,
203 as plotted in Figure 4a

$$\begin{aligned} \Omega_T(E_{\text{ext}}) = \Omega_T(0) \left[1 + \frac{8e^2}{\hbar\epsilon_0 k_B T} \left(\sqrt{mk_B T + \frac{e^2 \tau^2}{2} E_{\text{ext}}^2} - \right. \right. \\ \left. \left. \sqrt{mk_B T - \frac{e^2 \tau^2}{2} E_{\text{ext}}^2} \right) \right]^{-1/2} \end{aligned} \quad (6)$$

204 A comparison between our model and experimental results
205 is shown in Figure 4b,c. Fits were obtained assuming the
206 temperature of the Raman-active phonons rising linearly from

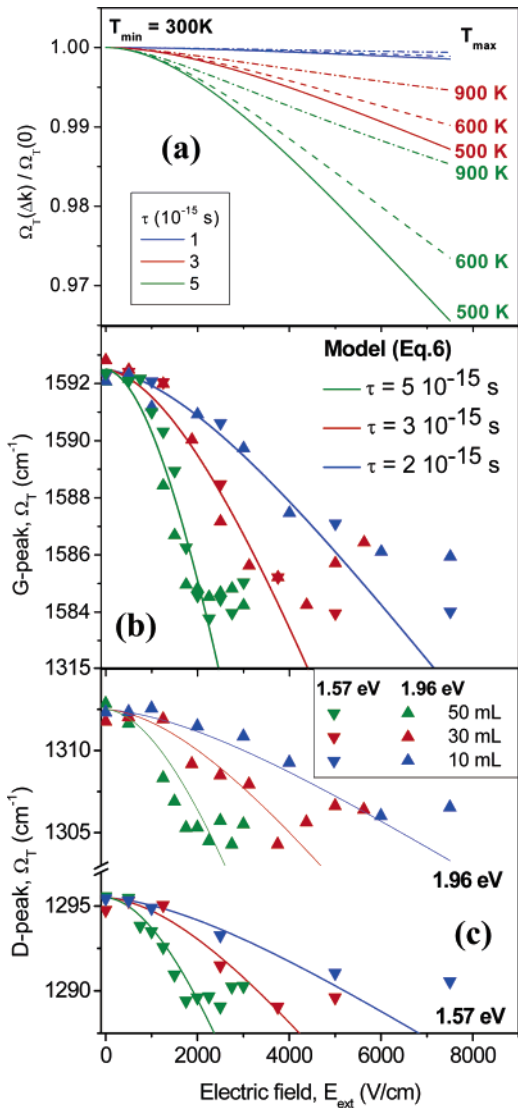


Figure 4. (a) Dependence of the Raman shifts on the electric field (E_{ext}) according to eq 6, assuming that the samples, initially at room temperature (T_{min}), heat proportionally with electric field (E_{ext}). Comparison with measured (b) G-peak and (c) D-peak frequencies. The lines represent data fits from eq 6 with $T_{max} = 600$ K and τ as reported in the legend.

207 $T_{min} = 300$ K to $T_{max} = 500$ – 700 K at external fields $E_{ext} =$
 208 0 – 7500 V/cm.²⁷ Note that these temperatures are far too
 209 low to burn the m-SWNTs. Furthermore, strong temperature
 210 increase would have been accompanied by broadening of
 211 the G, D, and RBM peaks,²⁶ which we did not observe. Thus
 212 Joule heating in our films must be moderate, in agreement
 213 with the relatively low maximum temperatures (T_{max}) pre-
 214 dicted by our model. In the framework of our model, the
 215 decrease in intensity of the Raman modes can be easily
 216 explained since the Stokes/anti-Stokes Raman cross sections
 217 $I_{S/AS} \sim |\partial\epsilon/\partial u_{||}|^2 + |\partial\epsilon/\partial u_{\perp}|^2$ ²⁸ decrease at increasing fields
 218 in direction longitudinal to the field, while remaining
 219 unchanged in transversal directions.^{29,30} Furthermore our fits
 220 lead to relaxation times of $\tau \sim (1$ – $5) \times 10^{-15}$ s, which agree
 221 well with the ones achievable by ellipsometry.² Such values
 222 are of the same order of magnitude to the inverse of the
 223 G-band pulsation ($t_G \approx 3 \times 10^{-15}$ s). This is in contrast to

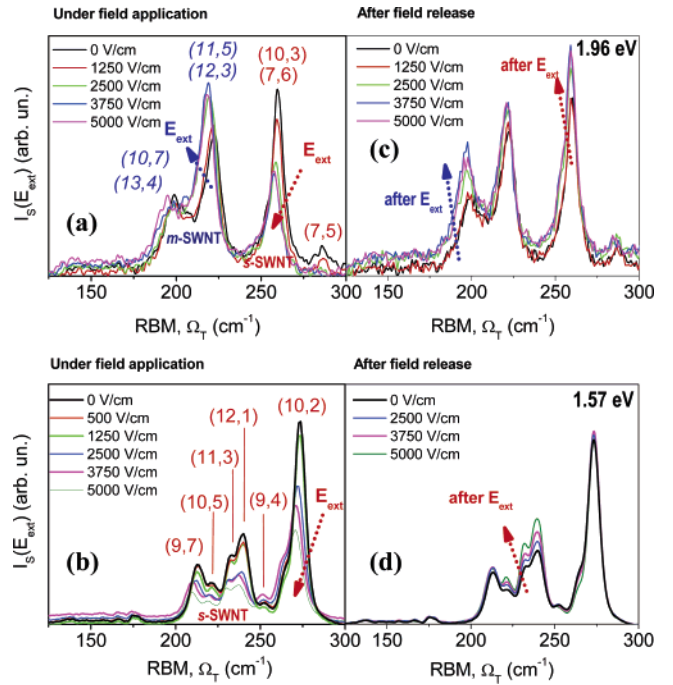


Figure 5. Modifications of the RBMs by external field at (a) 1.96 eV (exciting both m- and s-SWNTs) and (b) 1.57 eV (exciting only s-SWNTs). Assignments of specific (n,m)-SWNTs are taken from Telg et al.³² The reversible decrease for s-SWNTs (red) and the reversible increase for m-SWNTs (blue) are shown. In contrast, after field release, the permanent effects are always in increasing the RBM intensities for both s- and m-SWNTs at (c) 1.96 eV and (d) 1.57 eV.

224 what happens in a single graphene layer²⁰ (or, likely, a single
 225 individual m-SWNT) where the relaxation times, being
 226 dominated by intralayer (or intratube) processes, are much
 227 longer and $t_G \ll \tau \approx \tau_{INTRA} \approx 100 \times 10^{-15}$ s,³¹ leading to
 228 the breakdown of the adiabatic Born–Oppenheimer ap-
 229 proximation. In contrast, the condition $t_G \sim \tau \approx \tau_{INTER} \sim$
 230 10^{-15} s, which still persists in our thin films, leads to a
 231 scenario that is still adiabatic and, thus, entirely different
 232 from the nonadiabatic behavior of the Raman spectra in the
 233 presence of Kohn anomalies as discussed in ref 20.

234 We have also examined the RBMs of our thin films in
 235 order to investigate the influence of the electric field on
 236 (n,m)-SWNTs with various chiralities. The RBMs are shown
 237 in parts a and b of Figure 5. It can be seen from Figure 5a
 238 that at $\hbar\omega = 1.96$ eV, where both s- and m-SWNTs are
 239 excited, the intensities of the RBMs of s-SWNTs decrease
 240 with increasing electric field while the intensities of the
 241 RBMs of m-SWNTs increase. In Figure 5b ($\hbar\omega = 1.57$ eV)
 242 where only s-SWNTs are sampled, the intensities of the
 243 RBMs decrease with increasing electric field. In contrast,
 244 after the electric field has been released, it can be seen in
 245 Figure 5c,d that the RBM intensity always slightly increases
 246 in both s- and m-SWNTs. The most interesting feature of
 247 this slight increase is that it remains permanent subsequent
 248 to the field release. Thus, the decrease in measured conduc-
 249 tance shown in Figure 2d cannot be correlated to the claimed
 250 preferential elimination of m-SWNTs.

251 The increase in intensities of the RBMs of m-SWNTs is
 252 an expected effect if the increase in Boson number of the

optical phonons is the determining factor of peak intensity. The decrease in the intensities of RBMs in s-SWNTs is not consistent with Joule heating as the determining factor in controlling the intensity of the RBMs. Indeed, it can be demonstrated¹⁴ that the decrease in RBM intensities cannot be accounted for by assuming that all the m-SWNTs are moving closer to resonance, while all the s-SWNTs are moving off resonance. Upon a temperature increase, the resonant energies³² of some of our (n,m) -SWNTs are expected to be closer to the Raman excitation energies, 1.57 and 1.96 eV, while other (n,m) tubes will be farther from their resonant energies.¹⁴ However this would happen without any systematic dependency on the metallic or semiconducting nature of each (n,m) -SWNT.¹⁴ Rather, we suspect that the intensity decrease of the RBMs of s-SWNTs at increasing voltage are more likely to be related to the same causes determining the decrease of the D- and G-peak intensities.

In conclusion, we reported on the changes in Raman peaks of SWNT thin films as a function of an external electric field. We assign such effects to anomalous electron-phonon interactions. We dismiss the idea that, in SWNT thin films, voltage pulses produce Joule heating high enough to burn large amounts of m-SWNTs. This does not happen because the maximum temperatures reached in SWNT thin film devices under voltage application are much lower than in individual SWNT devices, and the relaxation times are much shorter. Rather, thermal oxidation,³³ selective cutting of the m-SWNTs, or elimination of very small amounts of m-SWNTs on some critical percolating pathways may reduce the “off” currents and improve the transistor performance. Finally, electrical Raman spectroscopy will be a new and powerful technique for characterizing thin films and devices incorporating one-dimensional nanostructures.

Supporting Information Available: Discussions of the difficulties of interpreting experiments in terms of electro-mechanical strain and the origin of the voltage dependency of the RBM intensities. This material is available free of charge via the Internet at <http://pubs.acs.org>.

References

- (1) Hu, L.; et al. *Nano Lett.* **2004**, *4*, 2513.
- (2) Fanchini, G.; et al. *Appl. Phys. Lett.* **2006**, *89*, 191919.
- (3) Dresselhaus, M. D.; Eklund, P. C. *Adv. Phys.* **2000**, *49*, 705.
- (4) Snow, E. S.; et al. *Appl. Phys. Lett.* **2003**, *82*, 2145.
- (5) Zhou, Y.; et al. *Nano Lett.* **2004**, *4*, 2031.

- (6) Seidel, R.; et al. *Nano Lett.* **2004**, *4*, 831. 297
- (7) Takenobu, T.; et al. *Appl. Phys. Lett.* **2006**, *88*, 033511. 298
- (8) Wu, Z.; et al. *Science* **2004**, *305*, 1273. 299
- (9) Unalan, H. E.; et al. *Nano Lett.* **2006**, *6*, 2513. 300
- (10) Thomsen, H.; Reich, S. *Phys. Rev. Lett.* **2000**, *85*, 5214. 301
- (11) Worlock, J. M.; Fleury, P. A. *Phys. Rev. Lett.* **1967**, *19*, 1176. 302
- (12) Corio, P.; et al. *Chem. Phys. Lett.* **2003**, *370*, 675; **2004**, *392* 396. 303
- Okazaki, K.; et al. *Phys. Rev. B* **2003**, *68*, 035434. 304
- (13) Hartman, A. Z.; et al. *Phys. Rev. Lett.* **2004**, *92*, 236804. 305
- (14) See Supporting Information. 306
- (15) Lazzeri, M.; et al. *Phys. Rev. Lett.* **2005**, *95*, 236802. 307
- (16) Piscanec, S.; et al. *Phys. Rev. Lett.* **2004**, *93*, 185503. 308
- (17) Ashcroft, N. W.; Mermin, N. D. *Solid State Physics*; Saunders: Philadelphia, 1976; p 323. 309
- (18) Dressel, M.; Gruner, G. *Electrodynamics of Solids*; Cambridge University Press: Cambridge, 2002. 311
- (19) Ferrari, A. C.; Robertson, *Phys. Rev. B* **2000**, *61*, 14095. 313
- (20) Pisana, S.; et al. *Nat. Mat.* **2007**, *6*, 198. See arXiv:cond-mat/0611714. 314
- (21) Popov, V. N.; Lambin, P. *Phys. Rev. B* **2006**, *73*, 085507. 315
- (22) Ashcroft, N. W.; Mermin, N. D. *Solid State Physics*; ref 17, 1976; p 316
515. 317
- (23) For instance, at $T = 0$ K, eq 3 would lead to $\epsilon(\Delta k, \hbar\omega) - 1 \sim \log\{[(x + 1)^2 - (x_E + y)^2]/[(x - 1)^2 - (x_E + y)^2]\}$, with $x = q/2k_F$, $x_E = \Delta k(E_{\text{ext}})/2k_F$, and $y = m\omega/\eta q$ so that Kohn anomalies ($x = 1$) correspond, in the absence of field, to an infinite static response $\epsilon(0,0) - 1 \rightarrow \infty$ and a null dynamic response $\epsilon(0, \hbar\omega) - 1 = 0$ while, in the presence of field, $\epsilon(\Delta k, 0) - 1 \rightarrow \infty$. 318
- (24) Actually, the use of the Lindhard model relies on the adiabatic Born-Oppenheimer approximation which, as verified below, still holds in our SWNT thin films. In contrast, our adiabatic model will be inadequate in nonadiabatic systems (e.g., graphene). 319
- (25) Ashcroft, N. W.; Mermin, N. D. Reference 22, pp 513–523. 320
- (26) Uchida, T.; et al. *Chem. Phys. Lett.* **2004**, *400*, 341. Zhou, Z.; et al. *J. Phys. Chem. B* **2006**, *110*, 1206. Nevertheless, while the changes achieved including possible anharmonic effects in our model are low, the influence on the electron screening of the alternating electric fields used for Raman excitation might also be considerable. This would suggest that our model might also be useful in explaining the temperature dependence of the Raman peaks of SWNT thin films in the absence of a constant external field. 321
- (27) The relaxation times determined within our model are of the order of magnitude available in literature (see ref 22, p 10). Furthermore, straightforward Drude analysis of the ellipsometry spectra of our samples (ref 2) also leads to $\tau \sim 10^{-15}$ s. We suspect that especially intertube processes between one m-SWNT and one s-SWNT are important in lowering the relaxation times, since s-SWNTs may act as thermal sink (ref 15). Thus, the higher the participation of s-SWNTs to electrical transport, the smaller τ_{INTER} . Impurities might also contribute in decreasing both intra- and intertube relaxation times. 322
- (28) u_{\parallel} and u_{\perp} represent, in each SWNT, the modes polarization longitudinal and transversal to the electric field. 323
- (29) Barker, A. S.; Loudon, R. *Rev. Mod. Phys.* **1972**, *44*, 18. 324
- (30) Fanchini, G.; et al. *J. Appl. Phys.* **2002**, *91*, 1155. 325
- (31) Zhang, Y.; et al. *Phys. Rev. Lett.* **2006**, *96*, 136806. 326
- (32) Telg, H.; et al. *Phys. Rev. Lett.* **2004**, *93*, 177401. 327
- (33) Jhi, S.-H.; et al. *Phys. Rev. Lett.* **2000**, *85*, 1710. 328

NL062418M

353